# Central peaks and Brillouin scattering in uniaxial relaxor single crystals of $Sr_{0.61}Ba_{0.39}Nb_2O_6$

F. M. Jiang,* J.-H. Ko, and S. Kojima†
*Institute of Materials Science, University of Tsukuba, Tsukuba, Ibaraki 305-8573, Japan*
(Received 6 August 2001; revised manuscript received 13 May 2002; published 13 November 2002)

The high-frequency dynamics of $Sr_{0.61}Ba_{0.39}Nb_2O_6$ are studied using the micro-Brillouin scattering technique to elucidate the uniaxial relaxor behavior. It is found that broad central peaks (CP's) appear at about 400 °C, which is much higher than the maximum temperature, $T_m \sim 72$ °C, of the dielectric constant along the unique polar *z* axis, and they remain down to −100 °C. The marked polarization dependence observed for CP's indicates that their origin is due to the thermally switching nano-size polar clusters whose polar axis is along the *z* axis. The CP intensity reveals a possible crossover from a high-temperature relaxor state to a low-temperature ferroelectric state. Brillouin frequency shifts and their linewidths indicate diffuse phase transition behavior around $T_m$. The temperature variation of the elastic constants $C_{11}$, $C_{33}$, and $C_{44}$ is determined, and $C_{33}$ and $C_{44}$ are found to exhibit marked changes around $T_m$.

DOI: 10.1103/PhysRevB.66.184301 PACS number(s): 78.35.+c, 77.80.Bh, 63.20.−e, 62.20.Dc

## I. INTRODUCTION

Elucidating the cluster dynamics of disordered ferroelectric systems poses challenging problems that have been studied during the past several decades, and many attempts have been made to understand the mechanisms they involve. Despite this effort, the nature of these dynamics remains largely unexplained. One important family of such disordered systems consists of relaxor ferroelectrics including lead magnesium niobate $Pb(Mg_{1/3}Nb_{2/3})O_3$ (PMN),[1] lead zinc niobate $Pb(Zn_{1/3}Nb_{2/3})O_3$ (PZN),[2] lanthanum doped lead zirconate titanate $La_xPb_{1-3x/2}(Zr_yTi_{1-y})O_3$ (PLZT),[3,4] and strontium barium niobate $Sr_{0.61}Ba_{0.39}Nb_2O_6$ (SBN).[5] One characteristic feature of this family is the existence of a frequency-dependent ''diffuse phase transition,'' for which the maximum temperature $T_m$ of the dielectric constant increases as the measuring frequency increases.[6] However, structure analysis has shown that no obvious macroscopic structural phase transition occurs in relaxor ferroelectrics.[7–10] Linear birefringence and strain measurements have revealed that precursor polar clusters appear below the Burns temperature $T_d$, which is much higher than $T_m$.[6,11–14] Various experiments carried out on PMN in zero field have provided some evidence that there is a crossover from a high-temperature superparaelectric phase to either ferroelectric nanodomain states stabilized by quenched random fields[11,15–18] or a dipolar glass state with random competing interactions.[19–22] In attempts to account for these results, various theoretical models have been proposed.[1,6,11,17–25]

$Sr_{0.61}Ba_{0.39}Nb_2O_6$, with $x \approx 0.61$ (SBN:61), is of interest with regard to both fundamental research on uniaxial relaxor ferroelectrics and applications,[5,6] due to its prominent pyroelectric,[5] electro-optic,[26,27] photorefractive[28–30] and nonlinear optic properties.[31] SBN belongs to the group of materials possessing an unfilled tungsten bronze structure with the general formula $AB_2O_6$—or, more correctly, $(A_1)_2(A_2)_4C_4(B_1)_2(B_2)_8O_{30}$—where *A* is a divalent or monovalent metal ion, *B* is either Nb or Ta, and C can be occupied only by very small metal ions, for example, Li ions. The crystal symmetry is tetragonal $4/mmm$ above $T_m$ and remains tetragonal ($4mm$) below $T_m$.[32] In SBN, the $A_1$ site is occupied solely by the smaller $Sr^{2+}$ (ionic radius 1.12 A), and the $A_2$ site is occupied by $Sr^{2+}$ and the larger $Ba^{2+}$ (with an ionic radius of 1.34 A), while the *C* site is empty. There are totally six *A* sites for five Sr+Ba atoms, and these sites are not fully occupied. Therefore, SBN has built-in disorder among the *A* sites.[32] Due to the uniaxial tunnel structures existing along the *c* axis, the difference between the ionic radii of $Ba^{2+}$ and $Sr^{2+}$ and built-in disorders, local random fields and polarizations are expected to exist along the *c* axis. Measurements of thermal properties, strain, and linear birefringence show that polar clusters appear below $T_d$, and these result in deviation from a linear temperature dependence.[6,12–14] The appearance of dielectric behavior indicates a poly-dispersive relaxation nature caused by the polar clusters.[33] Very recently, Dec *et al.* reported susceptibility related to polar clusters and birefringence induced by spontaneous and precursor polarizations in pure and $Ce^{3+}$-doped SBN:61. They concluded that relaxor behavior prevails in the precursor regime, where $T > T_m$, and a ferroelectric domain state is encountered for $T < T_m$.[34] The dependence of the critical exponents on the doping concentration of $Ce^{3+}$ near the phase transition point, which can be derived from the linear birefringence, indicates that Ce-doped SBN may approach the three-dimensions random-field Ising universality class.[35]

In contrast with normal ferroelectrics, no soft mode has been found in relaxor materials.[36] Raman bands are very broad, and the number of vibrational bands is far less than that of theoretically predicted normal modes.[37,38] Their dielectric constants are very large, but the LST relation does not hold in this case.[36,37] There might be some other mechanism able to cause large dielectric constants. Burns proposed two possible origins: relaxation and very low-frequency

 

overdamped soft optic modes.[37] Quasielastic light scattering is closely related to mesoscopic cluster dynamics,[39] and indeed fluctuations of precursor polar clusters result in central peaks (CP's). CP's have been reported in other disordered ferroelectric materials, such as $KTaO_3$ doped with small percentages of lithium at the *A* site or niobium at *B* sites. Disorder-induced first-order scattering and soft modes have been observed a few degrees both above and below $T_c$. As the origin of CP's, the coupling of soft optic modes to relaxation modes has been discussed.[39–42]

In this paper, we report on a low-frequency light scattering study of SBN:61 crystals using a high contrast micro-Brillouin scattering technique. Recently, we observed CP's in relaxor ferroelectric 0.65PMN-0.35PT,0.91PZN-0.09PT single crystals,[43,44] and also reported preliminary results on CPs in SBN:61 over a very wide temperature range.[45,46] To obtain more insight into the uniaxial relaxor behavior observed in SBN:61, detailed polarizing Brillouin spectra were compiled as functions of temperature in both cooling and heating processes, and possible origins of CP's were discussed. Diffuse phase transition behavior is illustrated by the use of the frequency shifts and their linewidths in the Brillouin spectra for different scattering geometries. To our knowledge, no Brillouin study of SBN has been previously reported.

## II. EXPERIMENT

Brillouin scattering spectra were measured using a high-resolution tandem Fabry-Perot interferometer combined with an optical microscope. A single-frequency $Ar^+$-ion laser was used to excite samples with a wavelength of 514.5 nm and a power of 50 mW. A conventional photon-counting system and a multichannel analyzer were used to detect and average the signal. Samples were placed in a cryostat cell (THMS 600) with temperatures varying from $-190$ to 600 °C and a stability of $\pm 0.1$ °C. The sample cell with *X*-*Y* adjustment was positioned on the stage of a reflection optical microscope (OLYMPUS BH-2). Brillouin scattering, combined with an optical microscope with a focal point of 1.3 $\mu$m, was found to be useful microprobe tool that enables us to investigate different microareas of the same size. The experimental setup was similar to that reported by Takagi and Kurihara.[47] $Sr_{0.61}Ba_{0.39}Nb_2O_6$ crystals of good optical quality were cut and polished. A backward scattering geometry was employed. A free spectral range (FSR) of 75 GHz was used to measure the frequency shifts and line width, and a FSR of 200 GHz was used to measure CP's.

TABLE I. Relations between the elastic constants and phase velocities of acoustic modes observed in Brillouin scattering. Here $\Delta\omega_B = 4\pi n/\lambda_0 v$, $n$ is the index, and $\lambda_0$ is the light wavelength in vacuum. The *x* and *y* axes are equivalent; $TA_1$ and $TA_2$ are degenerate.

| Geometry | Wave vector | LA | $Ta_1$ | $TA_2$ |
|---|---|---|---|---|
| $z(xx)\bar{z}$ | $q\|\|(001)$ | $\rho v_{LA_c^2} = C_{33}$ | × | × |
| $z(xy)\bar{z}$ | $q\|\|(001)$ | × | $\rho v_{TA1}^2 = C_{44}$ | $\times(\rho v^2 = C_{44})$ |
| $x(zz)\bar{x}$ | $q\|\|(100)$ | $\rho v_{LAa}^2 = C_{11}$ | × (QTA$_1$ leakage) | × |
| $x(yy)\bar{x}$ | $q\|\|(100)$ | $\rho v_{LAa}^2 = C_{11}$ | × | × |
| $x(zy)\bar{x}$ | $q\|\|(100)$ | × | × | × |

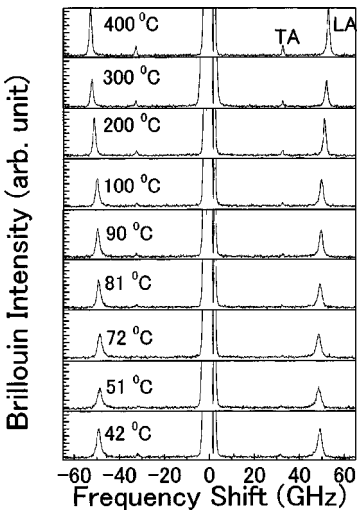


FIG. 1. Brillouin spectra at various temperatures for the backward scattering geometry $z(x,x+y)\bar{z}$.

## III. RESULTS

Typical Brillouin spectra on the *z*-plate with a scattering geometry $z(x,x+y)\bar{z}$ obtained at various temperatures are displayed in Fig. 1, where *x*, *y*, and *z* represent [100], [010], and [001] directions, respectively. Since SBN is tetragonal both above and below $T_m$,[32] the LA and TA modes propagating along the *z* axis are determined by $\rho v_L^2 = C_{33}$ and $\rho v_T^2 = C_{44}$, where $\rho$ is the density, $v_L$ and $v_T$ are the LA and TA mode velocities, respectively, and $C_{33}$ and $C_{44}$ are elastic stiffness constants (Table I).[48]

Figure 2 displays Brillouin spectra at room temperature on an *x* plate with different backward scattering geometries. The relations between the elastic constants and the LA and TA modes measured with different scattering geometries are summarized in Table I. Broad CP's of different intensities are

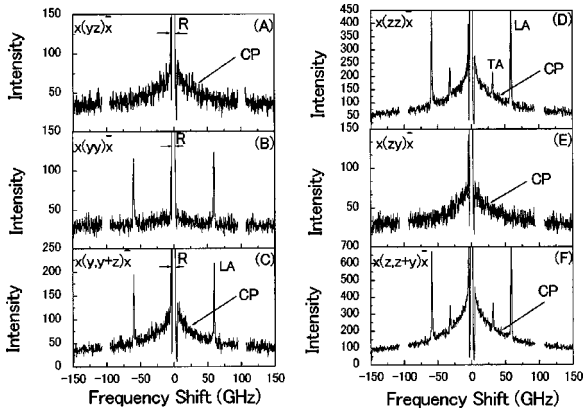


FIG. 2. Polarization dependences of Brillouin spectra measured for backward scattering geometries using an *x* plate.

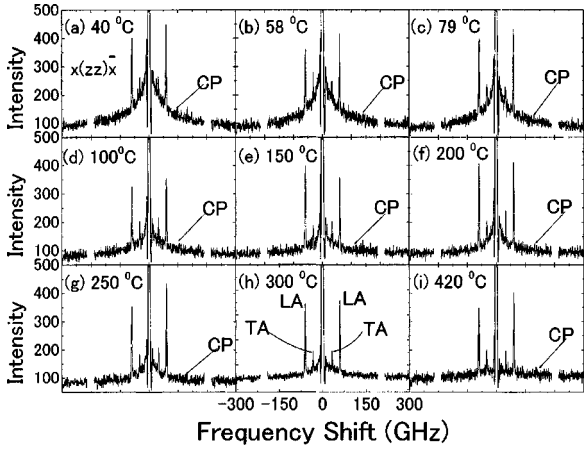


FIG. 3. Temperature dependence of Brillouin spectra for the scattering geometry of $x(zz)\bar{x}$.

observed for certain scattering geometries. The marked polarization dependence of the CP intensity indicates a uniaxial nature of SBN crystals. To make clear the origin of this polarization dependence, it is helpful to compare with Raman scattering results.

As we discuss in Sec. III, the broad CP is due to polarization fluctuations of the nano-size polar clusters orientated mainly along the unique polar *z* axis. To determine the thermal evolution of the CP accurately, a large FSR of 200 GHz and a scan range of 300 GHz–10 $cm^{-1}$ were used. The dependence on temperature of the CP in a cooling process is depicted in Figs. 3 and 4. An important feature of these plots is the broad CP that appears over a wide temperature interval of more than 400 °C. This kind of phenomena has never been observed in other disordered systems. Although generally, CP's may arise through different mechanisms,[39] they persist over only a narrow temperature range in the vicinity of phase transition temperatures.[40,41] Therefore, the phenomenon observed here for SBN is rather exceptional.

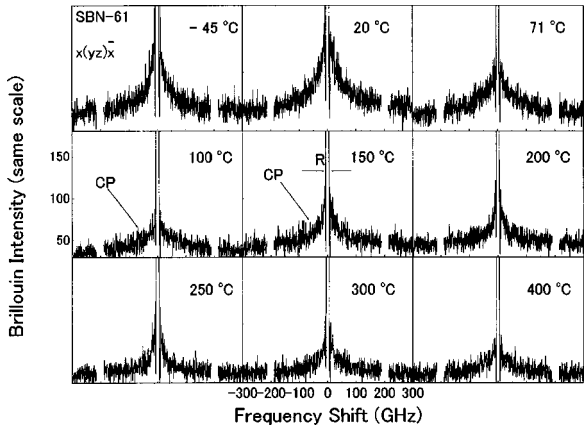


FIG. 4. Temperature dependence of Brillouin spectra for the scattering geometry of $x(zy)\bar{x}$.

TABLE II. Correspondence between vibrational mode species, Raman tensor components, and central peaks.

| Geometry | Raman mode | Tensor component | CP (intensity) |
|---|---|---|---|
| $x(zz)\bar{x}$ | $A_1(z)$(TO) | *b* | yes (strongest) |
| $x(zy)\bar{x}$ | $E(y)$(TO) | *e* | yes (intermediate strength) |
| $x(yz)\bar{x}$ | $E(y)$(TO) | *e* | yes (intermediate strength) |
| $x(yy)\bar{x}$ | $A_1(z)$(TO) | *a* | yes (very weak) |
| $z(xx)\bar{z}$ | $A_1(z)(\mathrm{LO})+B_1$ | *a,c* | no |
| $z(xy)\bar{z}$ | $B_2$ | *d* | no |

## IV. DATA ANALYSIS AND DISCUSSION

### A. Central peaks

$Sr_xBa_{1-x}Nb_2O_6$ $(0.25<x<0.75)$ is intrinsically disordered since there are totally six *A* sites for five ions ($Sr^{2+}+Ba^{2+}$), and the *A* sites are not fully occupied.[32] The $Sr^{2+}$ and $Sr^{2+}+Ba^{2+}$ ions are situated in distorted fourfold and fivefold tunnel-like structures along the *z* axis; there is positional disorder mainly along the *z*-axis for almost all ions. The differences between the intrinsic disorder and the ionic radii for $Sr^{2+}$ and $Ba^{2+}$ might be strong sources of random fields and local polarizations oriented essentially along the *z* axis.[34,35]

#### *1. Polarization dependence*

The broad bands in the Raman spectra of SBN clearly reflect the disordered nature of the crystal structure.[45] The excitations of primary interest are the $E(x,y)$- and $A_1(z)$-symmetry modes, which involve ionic motion perpendicular and parallel to the polar *z*-axis, respectively. Their corresponding Raman tensors are given by

$$R[A_1(z)]=\begin{pmatrix} a & & \\ & a & \\ & & b \end{pmatrix}, \quad R[E(x,y)]=\begin{pmatrix} & & e \\ & & e \\ e & e & \end{pmatrix},$$

$$R[B_1]=\begin{pmatrix} c & & \\ & -c & \\ & & \end{pmatrix}, \quad R[B_2]=\begin{pmatrix} & d & \\ d & & \\ & & \end{pmatrix}.$$

The compatibility relation between Raman and Brillouin scattering is summarized in Table II. The first column there lists scattering geometries, and to its right are the corresponding Raman modes. The third column lists the Raman tensor components corresponding to the intensities of the Raman modes observed with the same scattering geometry, and the last column lists the activity and relative intensities of the CP's.

It is clear from our results that CP's appear only in transverse optic (TO) mode spectra, and their intensities are closely related to the magnitude of Raman tensor components. From Raman scattering results,[45] it is concluded that

$R[A_1(z)]_{33}=b$ is the largest, $R[E(y)]_{23}=e$ is the second largest, and $a$ is the smallest. For $A_1(z)$(LO) mode spectra, it is reasonable that no CP appears, since the electric field of the incident light is perpendicular to the polarizations of the $A_1(z)$(LO) mode, and it cannot couple to $A_1(z)$(LO). $B_2$ is a nonpolar mode, and therefore there is no CP in the corresponding scattering geometry $z(xy)\bar{z}$. It is thus seen that polarizations or low-frequency polar modes might be one of the origins of the CP's. The significant polarization dependence of CP's indicates that this is first-order scattering. Since SBN is a uniaxial polar crystal with polarization mainly along the $z$ axis, it is reasonable that the CP is strongest for the $x(zz)\bar{x}$ scattering geometry, in which case the polar mode with polarization along the $z$-axis can couple to the field of the incident light. The relative intensities of CP's with different scattering geometries are in consistent with those reported by Wilde and Wilde in their Rayleigh scattering study of SBN:61.[49] However, they used a low resolution of 0.6 $cm^{-1}$, employing a double grating monochromator that provided only integrated intensities, indicating the possible appearance of CP's, and they did not elucidate the reason that marked polarization dependences exist.

Since CP's are very weak for the $x(yy)x$ geometry, only those observed for $x(zz)\bar{x}$ scattering geometry were analyzed. A very noteworthy feature is the broad CP that appears over a wide temperature interval of more than 400 °C, as shown in Figs 3 and 4. Similarly, CP's have been observed over wide temperature ranges for 0.65PMN-0.35PT relaxor single crystals and PLZT ceramics.[43–45] It is therefore reasonable to assume that such stable CP behavior results from characteristics common to relaxor ferroelectric materials in general.

#### *2. Mechanism causing central peaks*

In most cases, CP's have been observed using light scattering techniques near phase transitions in a variety of systems. The conjectured mechanisms responsible for CP's include entropy fluctuations, phonon density fluctuations, dipolar relaxations, molecular reorientations, overdamped soft modes, and their coupling with vibration and relaxation modes, dynamic and static clusters, and domains, as well as a host of phenomena related to impurities, vacancies, etc.[39] Some of these conjectured mechanisms are first order and some are second order.[42] Entropy fluctuations can be excluded as a cause of the broad CP's, because they exist over a relatively narrow range (less than 1 GHz). Although molecular reorientations usually exist in organic solids and liquids, there is no rotational molecule in SBN. The remaining possible mechanisms responsible for the CP's are relaxations of clusters, domains, and a host of impurities and vacancies. Since the CP's exhibit a marked temperature dependence, static effects should fall within a relatively narrow frequency range, of order 1 GHz, and therefore they can be excluded as a mechanism involved in the broad CP.

In the present case of SBN, a CP appears at a temperature near 400 °C, much higher than $T_m$, and remains down to a very low temperature of about −100 °C in the cooling process. Because this behavior is unusual, we studied SBN previously using Raman scattering.[45,50] In that study, no soft mode was observed, and all the modes were relatively broad, due to the disordered nature of SBN. Therefore, soft modes and related couplings can be ignored in the situation studied presently. Judging from the polarization dependence of the Brillouin spectra, we believe that the CP is related to polarization fluctuations along the $z$ axis. Actually, the existence of precursor nanosize polar clusters has been confirmed by linear refractive index and birefringence and strain measurements in SBN-60, and a Burns temperature of $T_d \sim 300$ °C, at which nanosize polar clusters appear, was deduced.[12,13,35] As the CP's in light scattering may be a direct reflection of the polarization fluctuations of nanosize polar clusters along the $z$-axis, the marked growth in intensity below $T_d$ indicates an increase in the volume or number density of nano-size polar clusters and an increase in the magnitude of local polarizations. These types of behavior are consistent with the detectable deviation from linear temperature dependences of the thermal strain and refractive index observed previously[12,13,35]

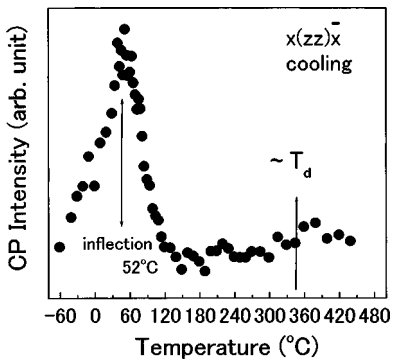


FIG. 5. Temperature dependence of the integrated intensity of the CP during the cooling process with the scattering geometry of $x(zz)\bar{x}$.

#### *3. Temperature dependence of central peaks*

The integrated intensity of CP during cooling in the case of the $x(zz)\bar{x}$ scattering geometry is displayed in Fig. 5. The rapid increase seen above $T_c$ may result from the increase in density of precursor nanosize polar clusters, while the decrease below $T_c$ may be caused by the growth of macroscopic ferroelectric domains. If this is indeed the case, then the CP intensity showed decrease markedly and exhibit thermal hysteresis once the sample is poled. Wilde and Wilde studied Rayleigh scattering of SBN:61 single crystals using a double monochromator.[49] They reported strong Rayleigh scattering for unpoled samples and a marked decrease in Rayleigh scattering for poled samples. In addition, the maximum temperatures they reported for Rayleigh scattering intensities are lower than $T_m$ for both heating and cooling processes. The reason for such a temperature difference is still not clear. It might be due to the increase of polarization fluctuations in the vicinity of surfaces of growing polar clusters.

### B. Diffuse phase transition

Frequency shifts and the full width at half maximum (FWHM) in the Brillouin spectra are very sensitive to phase

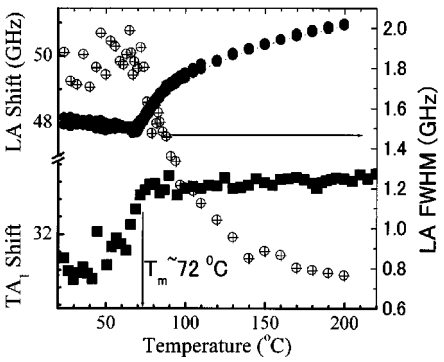


FIG. 6. Temperature dependences of Brillouin frequency shift LA (filled circles) and TA modes (filled squares), and the FWHM of LA modes (open circles with crosses) for the $z(x,x+y)\bar{z}$ geometry.

transitions, and the frequency shifts are related to elastic constants for certain acoustic modes. Acoustic modes observed with different scattering geometries and related elastic constants are listed in Table I. To extract quantitative information from the Brillouin spectra, we first consider the spectra on a *z* plate. In this case there is no CP, and therefore we used a simple damped harmonic oscillator model to fit the LA and $TA_1$ modes. Since the $TA_1$ mode is relatively weak, only frequency shifts of the $TA_1$ modes were derived. The frequency shifts of the LA and $TA_1$ modes, and the FHWM of the LA mode are plotted in Fig. 6. It is seen that the LA and $TA_1$ mode frequency shifts for $q\|(001)$ change continuously with temperature. A broad dip in the LA shifts and a slow drop in $TA_1$ shifts are found near 72 °C in the cooling process. These results are in agreement with temperature variation of the dielectric constant, which has a peak around 72 °C and is diffusive in nature. The frequency shifts of LA and $TA_1$ modes for $q\|(100)$ on an *x* plate are displayed in Fig. 7, where $TA_1$ is forbidden by symmetry (Table I). It is found that this $TA_1$ is strongly anisotropic, and it is attributed to a leakage of the $TA_1$ mode, because it exhibits behavior similar to that of $TA_1$ displayed in Fig. 6. The frequency shifts of the LA modes on the *x* plate decrease continuously during cooling, and no abrupt change or anomaly is found near $T_m$. Such a continuous change is typical for relaxor ferroelectrics.[51–53]

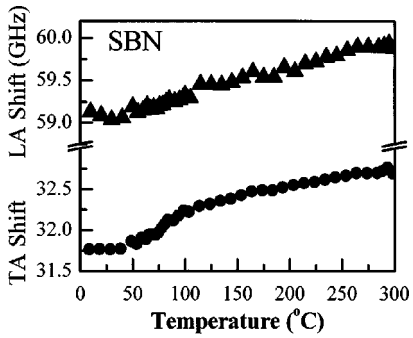


FIG. 7. Temperature dependences of frequency shifts for LA (top) and $TA_1^*$ (bottom) modes measured at backward scattering geometries using an *x* plate.

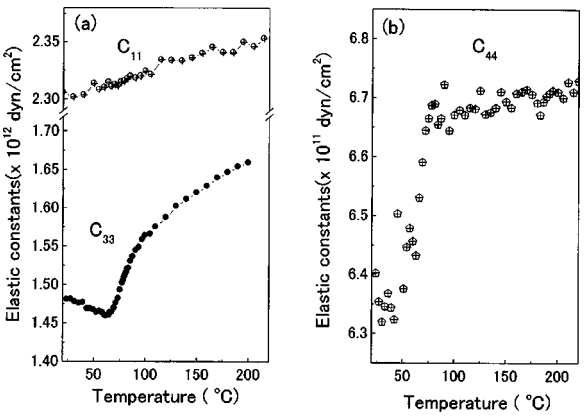


FIG. 8. Temperature dependences of elastic constants determined using Brillouin scattering.

### C. Elastic stiffness constants: $C_{11}$, $C_{33}$, $C_{44}$

Using the values of the refractive index, elastic stiffness constants can be calculated from the measured Brillouin frequency shifts. In the case of backward Brillouin scattering the frequency shift $f_B$ is given by $f_B = 2nv/\lambda_0$, where *n* and *v* are the associated refractive index and the phase velocity of acoustic waves, respectively. Thus the elastic constants are given by

$$C_{33} = \rho v_{\mathrm{LA}}^2(001) = \rho\left[\frac{f_{\mathrm{LA}}(q\|001)\lambda_0}{2n_0}\right], \tag{1}$$

$$C_{11} = \rho v_{\mathrm{LA}}^2(100) = \rho\left[\frac{f_{\mathrm{LA}}(q\|100)\lambda_0}{2n_e}\right], \tag{2}$$

$$C_{44} = \rho v_{\mathrm{TA}}^2(001) = \rho\left[\frac{f_{\mathrm{TA}}(q\|001)\lambda_0}{2n_0}\right], \tag{3}$$

where $\rho$, $n_0$, and $n_e$ are the density and the ordinary and extraordinary refractive indices, respectively. The value of $\rho$ is calculated theoretically to be 5.3 g/cm$^3$, using the lattice parameters in the literature.[31] The values of $n_o$ and $n_e$ for SBN61 are taken to be 2.3684 and 2.3333 at a wavelength of 514.5 nm, as found in the literature.[54] The calculated temperature dependences of the elastic constants are plotted in Fig. 8. The room temperature values are $C_{11} \sim 23.0\times10^{11}$, $C_{33} \sim 14.8\times10^{11}$, and $C_{44} \sim 6.38\times10^{11}$ dyn/cm$^2$. These values are similar to those found for $Sr_{0.6}Ba_{0.4}Nb_2O_6$ measured with the piezo-resonance method,[55] $C_{11}^E \sim 24.7\times10^{11}$, $C_{11}^D \sim 25.4\times10^{11}$, $C_{33}^E \sim 13.2\times10^{11}$, $C_{33}^D \sim 16.2\times10^{11}$, $C_{44}^E \sim 6.46\times10^{11}$, and $C_{44}^D \sim 6.94\times10^{11}$ dyn/cm$^2$.

## V. CONCLUSION

We reported what we believe to be the first micro-Brillouin scattering study of SBN:61 single crystals. Marked polarization and temperature dependences of CP's were observed, and they are attributed to polarization fluctuations and domain wall dynamics. Local polarizations are oriented

mainly along the unique polar *z* axis, but they have weak components within the plane perpendicular to the *z* axis. This reveals that CPs are closely related to fluctuations of nanosize polar clusters. Because SBN is uniaxial, the intensities of CP's are different for different scattering geometries. It was found that they are strongest for the $x(zz)\bar{x}$ scattering geometry. The possible crossover from a high temperature relaxor phase to a low temperature ferroelectric state is reflected in the temperature dependence of the integrated intensity of the CP's. Brillouin frequency shifts and linewidths exhibit a diffusive nature around 72 °C. Finally, the temperature dependences of elastic constants were determined accurately.

## ACKNOWLEDGMENTS

This work was supported in part by a Grant-in-Aid for scientific research (B), No. 10440115 from JSPS, and research grants from the Japan Sheet Glass Foundation and the Marubun Research Promotion Foundation. The authors are grateful to Professor W. Kleemann, Professor M. S. Jang, and Dr. S. Lushnikov for fruitful discussions.

*Present address: Department of Geoscience, Princeton University, Princeton, NJ 08544.

†Author to whom all correspondence should be addressed. Email address: kojima@bk.tsukuba.ac.jp

[1] V. A. Bokov and I. E. Myl'nikova, Fiz. Tverd. Tela (Leningrad) **3**, 841 (1961) [Sov. Phys. Solid State **3**, 613 (1961)].

[2] J. Kuwata and K. Uchino, and S. Nomura, Ferroelectrics **22**, 863 (1979).

[3] Y. Xi, C. Zhili, and L. E. Cross, J. Appl. Phys. **54**, 3399 (1983).

[4] S. Kamba, V. Bovtun, J. Petzelt, I. Rychetsky, R. Mizaras, A. Brilingas, J. Banys, J. Grigas, and M. Kosec, J. Phys.: Condens. Matter **12**, 497 (2000).

[5] A. M. Glass, J. Appl. Phys. **40**, 4699 (1969).

[6] L. E. Cross, Ferroelectrics **76**, 241 (1987).

[7] N. de Mathan, E. Husson, G. Calvarin, J. R. Gavarri, A. W. Hewat, and A. Morell, J. Phys.: Condens. Matter **3**, 8159 (1991).

[8] P. Bonneau, P. Garnier, G. Calvarin, E. Husson, J. R. Gavarri, A. W. Hewat, and A. Morell, J. Solid State Chem. **91**, 350 (1991).

[9] S. Vakhrushev, S. Zhukov, G. Fetisov, and V. Chernyshov, J. Phys.: Condens. Matter **6**, 4021 (1994).

[10] N. de Mathan, E. Husson, G. Calvarin, and A. Morell, Mater. Res. Bull. **26**, 1167 (1991).

[11] W. Westphal and W. Kleemann, Phys. Rev. Lett. **68**, 847 (1992).

[12] A. S. Bhalla, R. Guo, L. E. Cross, G. Burns, F. H. Dacol, and Ratnakar R. Neurgaonkar, Phys. Rev. B **36**, 2030 (1987).

[13] G. Burns and F. H. Dacol, Phys. Rev. B **28**, 2527 (1983).

[14] J. J. De. Yoreo, R. O. Pohl, and G. Burns, Phys. Rev. B **32**, 5780 (1985).

[15] Z.-Y. Cheng, L.-Y. Zhang, and X. Yao, J. Appl. Phys. **79**, 8615 (1996).

[16] Z.-Y. Cheng, R. S. Katiyar, X. Yao, and A. Guo, Phys. Rev. B **55**, 8165 (1997).

[17] Z.-Y. Cheng, R. S. Katiyar, X. Yao, and A. S. Bhalla, Phys. Rev. B **57**, 8166 (1998).

[18] A. E. Glazounov and A. K. Tagantsev, J. Phys.: Condens. Matter **10**, 8863 (1998).

[19] D. Viehland, S. J. Jang, L. E. Cross, and M. Wuttig, J. Appl. Phys. **68**, 2916 (1990).

[20] D. Viehland, S. J. Jang, L. E. Cross, and M. Wuttig, J. Appl. Phys. **69**, 6595 (1991).

[21] D. Viehland, S. J. Jang, L. E. Cross, and M. Wuttig, Phys. Rev. B **46**, 8003 (1992).

[22] D. Viehland, F. J. Li, S. J. Jang, L. E. Cross, and M. Wuttig, Phys. Rev. B **46**, 8013 (1992).

[23] D. Viehland, F. J. Li, S. Jang, L. E. Cross, and M. Wuttig, Philos. Mag. B **64**, 335 (1991).

[24] A. K. Tagantsev and A. E. Glazounov, Phys. Rev. B **57**, 18 (1998).

[25] A. Bell, J. Phys.: Condens. Matter **5**, 8773 (1993).

[26] K. Tada, T. Murai, A. Aoki, K. Muto, and K. Awazu, Jpn. J. Appl. Phys. **11**, 1622 (1972).

[27] R. R. Neurgaonkar, W. K. Cory, and J. R. Oliver, Ferroelectrics **51**, 3 (1983).

[28] B. Fisher, M. Cronin-Golomb, J. O. White, A. Yariv, and R. R. Neurgaonkar, Appl. Phys. Lett. **40**, 863 (1982).

[29] G. Salamon, M. J. Miller, W. W. Clark III, G. L. Wood, and E. J. Sharp, Opt. Commun. **59**, 417 (1986).

[30] R. R. Neurgaonkar, W. K. Cory, J. R. Oliver, M. D. Ewbank, and W. F. Hall, Opt. Eng. (Bellingham) **26**, 392 (1987).

[31] S. C. Abrahams, P. B. Jamieson, and J. L. Bernstein, J. Chem. Phys. **54**, 2355 (1971).

[32] P. B. Jamieson, S. C. Abrahams, and J. L. Bernstern, J. Chem. Phys. **48**, 5048 (1968).

[33] Z. G. Lu and G. Calvarin, Phys. Rev. B **51**, 2694 (1995).

[34] J. Dec, W. Kleemann, Th. Woike, and R. Pankrath, Eur. Phys. J. B **14**, 627 (2000).

[35] P. Lehnen, W. Kleemann, Th. Woike, and R. Pankrath, Eur. Phys. J. B **14**, 637 (2000).

[36] M. E. Line and A. M. Glass, *Principles and Applications of Ferroelectrics and Related Materials* (Clarendon Press, Oxford, 1977), Chap. 8.

[37] G. Burns, J. D. Axe, and D. F. O'Kane, Solid State Commun. **7**, 933 (1969).

[38] S. D. Ross, J. Phys. C **3**, 1785 (1970).

[39] P. A. Fleury and K. B. Lyons, in *Light Scattering Near Phase Transitions*, edited by H. Z. Cummins and A. P. Levanyuk (North-Holland, Amsterdam, 1983), Chap. 7, p. 449.

[40] K. B. Lyons, P. A. Fleury, and D. Rytz, Phys. Rev. Lett. **57**, 2207 (1986).

[41] Edward Lee, L. L. Chase, and L. A. Boatner, Phys. Rev. B **31**, 1438 (1985).

[42] B. E. Vugmeister, Y. Yacoby, J. Toulouse, and H. Rabitz, Phys. Rev. B **59**, 8602 (1999).

[43] F. M. Jiang and S. Kojima, Phys. Rev. B **62**, 8572 (2000).

[44] F. M. Jiang and S. Kojima, Appl. Phys. Lett. **77**, 1271 (2000).

[45] F. M. Jiang and S. Kojima, Jpn. J. Appl. Phys., Part 1 **39**, 5704 (2000).

[46] S. Kojima and F. M. Jiang, in *Fundamental Physics of Ferroelectrics 2001*, edited by H. Krakauer, AIP Conf. Proc. No. 582 (AIP, New York, 2001), p. 61.

[47] Y. Takagi and K. Kurihara, Rev. Sci. Instrum. **63**, 5552 (1992).

[48] R. Vacher and L. Boyer, Phys. Rev. B **6**, 639 (1972).

[49] J. P. Wilde and R. E. Wilde, J. Appl. Phys. **71**, 418 (1992).
[50] S. Kojima and T. Nakamura, Ferroelectrics **25**, 589 (1980).
[51] W. F. Oliver, C. A. Herbst, S. M. Lindsay, and G. H. Wolf, Rev. Sci. Instrum. **63**, 1884 (1992).
[52] J. Habasaki and Y. Hiwatari, Phys. Rev. E **62**, 8790 (2000).
[53] L. A. Bursill and P. J. Lin, Philos. Mag. B **54**, 157 (1986).
[54] Th. Woike, T. Granzow, U. Dorfler, Ch. Poetsch, M. Wohlecke, and R. Pankrath, Phys. Status Solidi A **186**, R13 (2001).
[55] R. R. Neyrgaonkar and L. Cross, Mater. Res. Bull. **21**, 893 (1986).